Toward Improved Description of DNA Backbone: Revisiting Epsilon and Zeta Torsion Force Field Parameters.

In the Cornell et al. force field, the total energy is a sum of the bond stretching (E_{bond}), angle bending (E_{angle}), dihedral (E_{dih}), nonbonded electrostatic (E_{elst}), and nonbonded van der Waals (E_{vdW}) terms (eq S1).

$$E = E_{bond} + E_{angle} + E_{dih} + E_{elst} + E_{vdW} \tag{S1}$$

The dihedral term is described as a cosine series (eq S2), where n is the periodicity of the torsion, Vn is the rotational barrier, ϕ is the torsion angle, and γ is the phase angle.

$$E_{dih} = \sum_{torsions} \sum_{n} \frac{V_n}{2}[1 + \cos(n\phi - \gamma)] \tag{S2}$$

Table S1. The final $\varepsilon\zeta_{OL1}$ torsion parameters. C7 is a new atom type introduced to distinguish various angle CT-CT-OS-P in NA's backbone. Only parameters for CT-C7-OS-P (C2'-C3'-OS-P and C4'-C3'-OS-P) components of the ε angle were changed and parameters for H1-C7-OS-P (H3'-C3'-OS-P) component are the same as in ff99bsc0.

	Torsion		ε/ζ parameters	
		n	$V_n/2$	γ
ε	CT-C7-OS-P (C4'-C3'-O3'-P +C2'-C3'-O3'-P)	3	0.1526	162.5
		2	0.6468	139.8
		1	1.7749	205.9
ζ	C7-OS-P-O2 (C3'-O3'-P-O1P + C3'-O3'-P-O2P)	3	0.2941	358.3
	OS-P-OS-C7 (O5'-P-O3'-C3')	3	0.2941	358.3
	OS-P-OS-C7	2	0.9743	350.9
	OS-P-OS-C7	1	0.9289	1.8

Table S2. Average helical twist [°] for the individual base pair steps (terminal base pair steps are not included). Parameters are averaged over 50ns windows. 95% confidence intervals (not standard deviations) are given in the last rows in order to facilitate comparison.

time interval (ns)	GC/GC	CG/CG	GA/TC	AA/TT	AT/AT	TT/AA	TC/GA	CG/CG	GC/GC
ff99bsc0									
200-250	34.3	28.7	36.1	34.8	32.5	34.8	35.2	32.7	33.7
250-300	33.9	28.3	36.3	34.8	32.6	34.4	35.8	32.2	33.0
300-350	36.4	28.6	35.9	34.6	32.9	35.2	36.2	32.3	32.2
350-400	34.1	26.5	37.2	34.8	32.6	34.9	35.9	33.9	30.8
400-450	24.6	33.2	35.5	35.1	32.5	34.8	35.9	32.6	32.0
450-500	32.4	28.6	36.1	34.8	32.3	34.7	35.5	33.0	31.9
500-550	30.5	28.6	37.0	35.1	32.7	34.8	36.3	32.1	32.3
550-600	34.0	24.8	37.6	34.8	32.7	35.1	36.0	32.4	32.1
600-650	33.0	25.2	38.0	35.0	32.7	35.2	34.5	33.6	32.4
650-700	32.7	25.5	37.8	34.8	32.5	34.9	36.3	31.4	32.6
700-750	32.1	26.3	37.7	35.3	32.6	35.0	40.6	26.1	39.6
750-800	33.7	28.6	36.6	34.7	32.6	34.7	36.1	33.6	32.3
800-850	33.8	28.2	36.6	34.9	32.6	34.8	35.6	33.9	30.1
850-900	31.7	28.9	36.5	34.9	32.5	34.8	35.9	32.6	31.5
900-950	33.0	31.5	36.4	34.7	32.6	35.0	36.3	32.2	32.3
950-1000	32.5	32.3	35.8	34.7	32.4	34.8	36.0	32.8	32.1
average	32.7±1.2	28.4±1.2	36.7±0.4	34.9±0.1	32.6±0.1	34.9±0.1	36.1±0.6	32.8±0.9	33.6±1.0
ff99bsc0εζ_{OL1}									
200-250	32.5	35.5	36.0	35.6	32.9	35.7	36.1	35.1	32.1
250-300	31.4	35.5	36.2	36.0	33.0	36.3	35.4	35.9	31.6
300-350	31.7	36.1	35.7	36.4	32.9	36.0	36.5	35.0	32.4
350-400	31.7	35.9	36.0	36.0	32.9	36.0	35.6	35.6	31.9
400-450	32.2	35.1	35.8	36.3	32.9	36.0	36.0	34.3	32.5
450-500	32.1	35.1	36.1	35.5	32.9	35.6	36.2	35.4	32.0
500-550	32.0	35.6	36.3	35.7	32.9	36.0	35.6	35.9	31.9
550-600	31.9	35.6	36.0	36.1	32.9	35.8	36.1	35.6	31.8
600-650	31.4	35.6	34.8	36.9	32.9	35.9	36.0	35.5	31.7
650-700	32.1	34.9	36.1	35.9	33.1	36.0	35.7	35.9	32.0
700-750	34.6	34.4	35.8	35.9	33.1	35.7	35.9	35.2	31.9
750-800	35.3	33.8	35.7	35.9	33.0	36.0	35.9	35.5	31.9
800-850	33.8	33.1	36.3	36.0	32.9	36.0	35.5	36.1	31.7
850-900	31.9	35.3	35.6	35.9	32.9	35.6	36.6	34.8	32.1
900-950	32.2	35.7	36.3	35.8	32.9	35.6	36.2	35.5	31.9
950-1000	31.8	35.8	35.4	36.1	33.0	36.0	36.2	35.1	31.9
average	32.4±0.6	35.2±0.4	35.9±0.2	36.0±0.2	32.9±0.1	35.9±0.1	36.0±0.2	35.4±0.2	32.0±0.1

Figure S1. BI (ε_{BI} = 180º, ζ_{BI} = 270º) and BII (ε_{BII} = 270º, ζ_{BII} = 180º) backbone substates on the model structure.
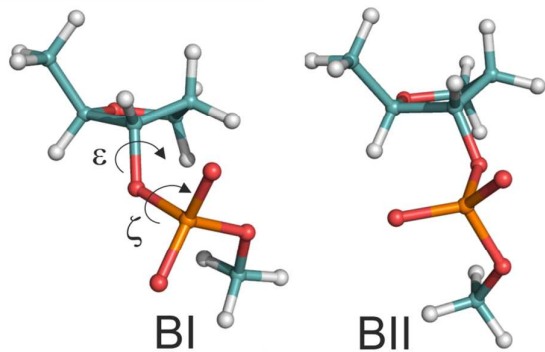
**Figure S2.** Comparison of the $\varepsilon\zeta_{OL}$ (red) and ff99bsc0 (blue) results with the QM reference (black) for selected points on the ε/ζ 2D surface for the model system shown in Figure 2. All energies are normalized to the canonical minimum (ε = 180°, ζ = 270°). Energies correspond to partially relaxed geometries where we adopted the same constraints for the partially relaxed optimizations as those adopted for deriving the torsion parameters. All calculations include solvation energy (QM/COSMO or MM/PB). The biggest deviation from the QM hypersurface is found for the ε/ζ = 180°/180° point, but this probably cannot be avoided within the framework of the separable ε/ζ torsion potentials.
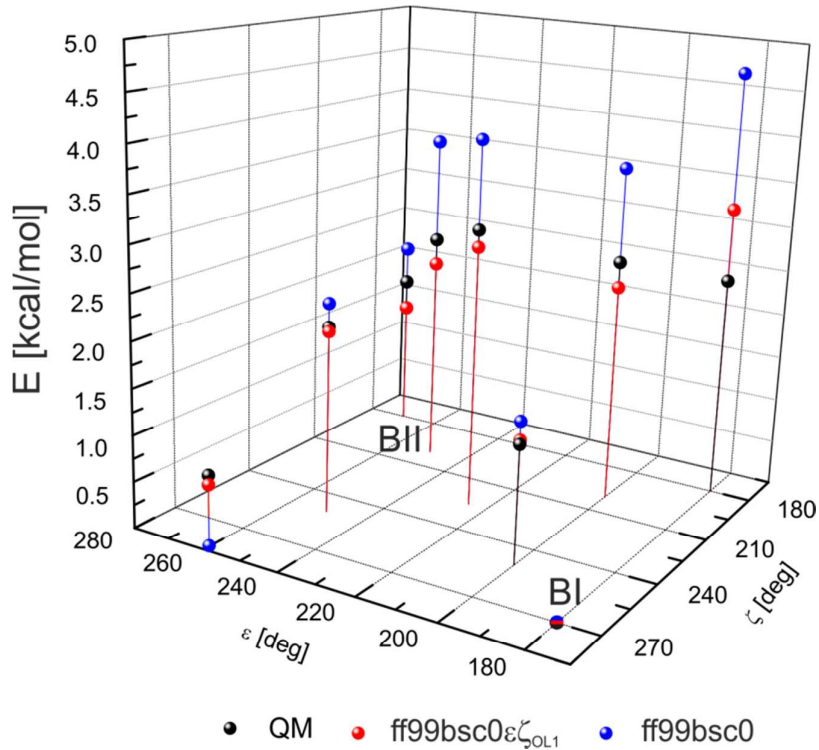
**Figure S3.** 2D ε/ζ potential energy surface obtained with QM (top, MP2/cc-pVTZ), ff99bsc0εζ$_{OL1}$ (middle) and ff99bsc0 (bottom) for the model system shown in Figure 2. Geometries were optimized at PBE/6-311++G(3df,3pd)-D/COSMO level and all dihedrals were fully relaxed. Solvation energy is included (COSMO/PBE/6-311++G(3df,3pd) in QM and PB in MM). All energies are in kcal/mol. Note that this level of theory is somewhat lower than that used for parameter derivation (MP2/CBS), therefore the results are not fully comparable. Heights of the barriers between BI and BII minima predicted by QM and ff99bsc0εζ$_{OL1}$ are lower than those obtained with ff99bsc0 force field.
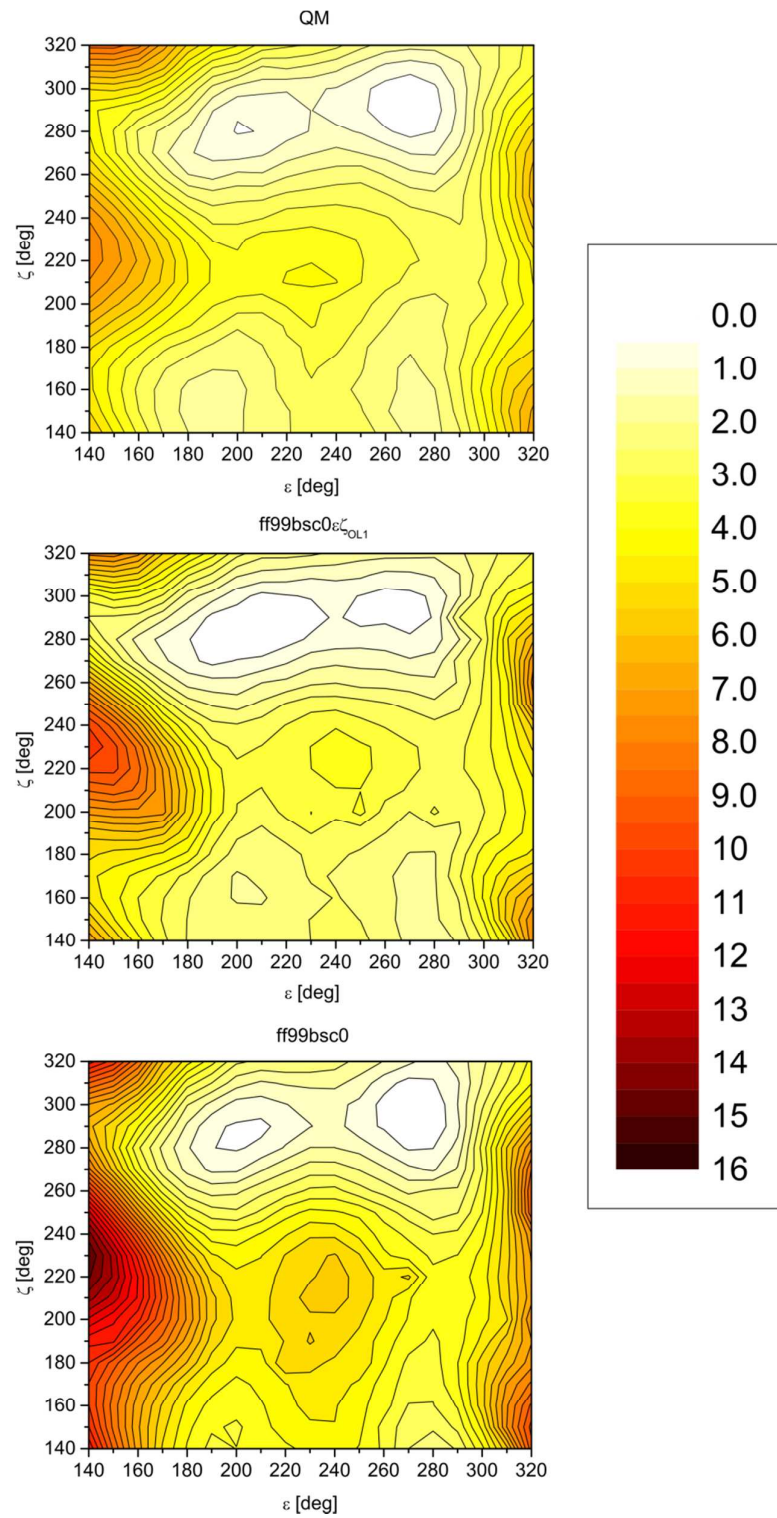
**Figure S4:** ε/ζ energy landscape derived from the X-ray database data through Boltzmann formula. Energy is plotted as a function of the ε - ζ coordinate. BI state corresponds to ε - ζ around -90° and BII to ε - ζ around +90°. Temperature of 175 K was considered in the Boltzmann formula because most crystal structures are determined at low temperatures.
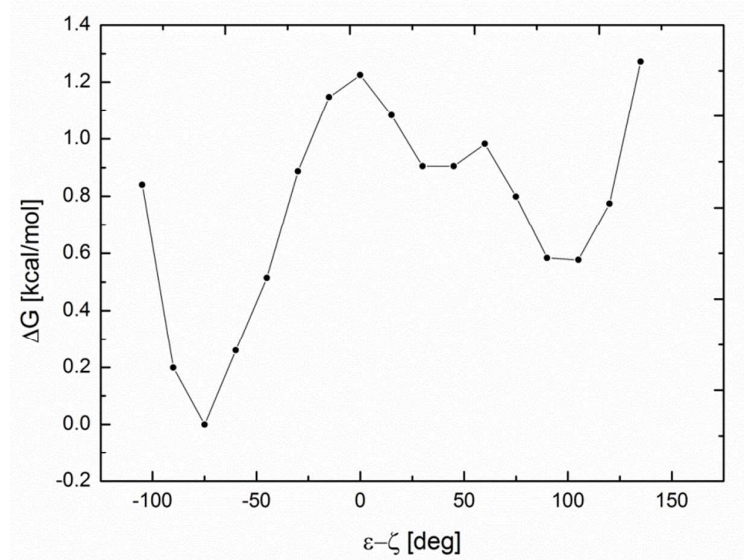
Figure S5. Distribution of backbone angles and sugar pucker observed in X-ray structures (blue, noncomplexed B-DNA structures only) and MD simulations with ff99bsc0 (black) and ff99bsc0εζ_{OL1} (red) force fields. Data were derived from the last 800 ns of the 1 μs simulations of DD dodecamer, excluding the last two terminal base pairs at each end.
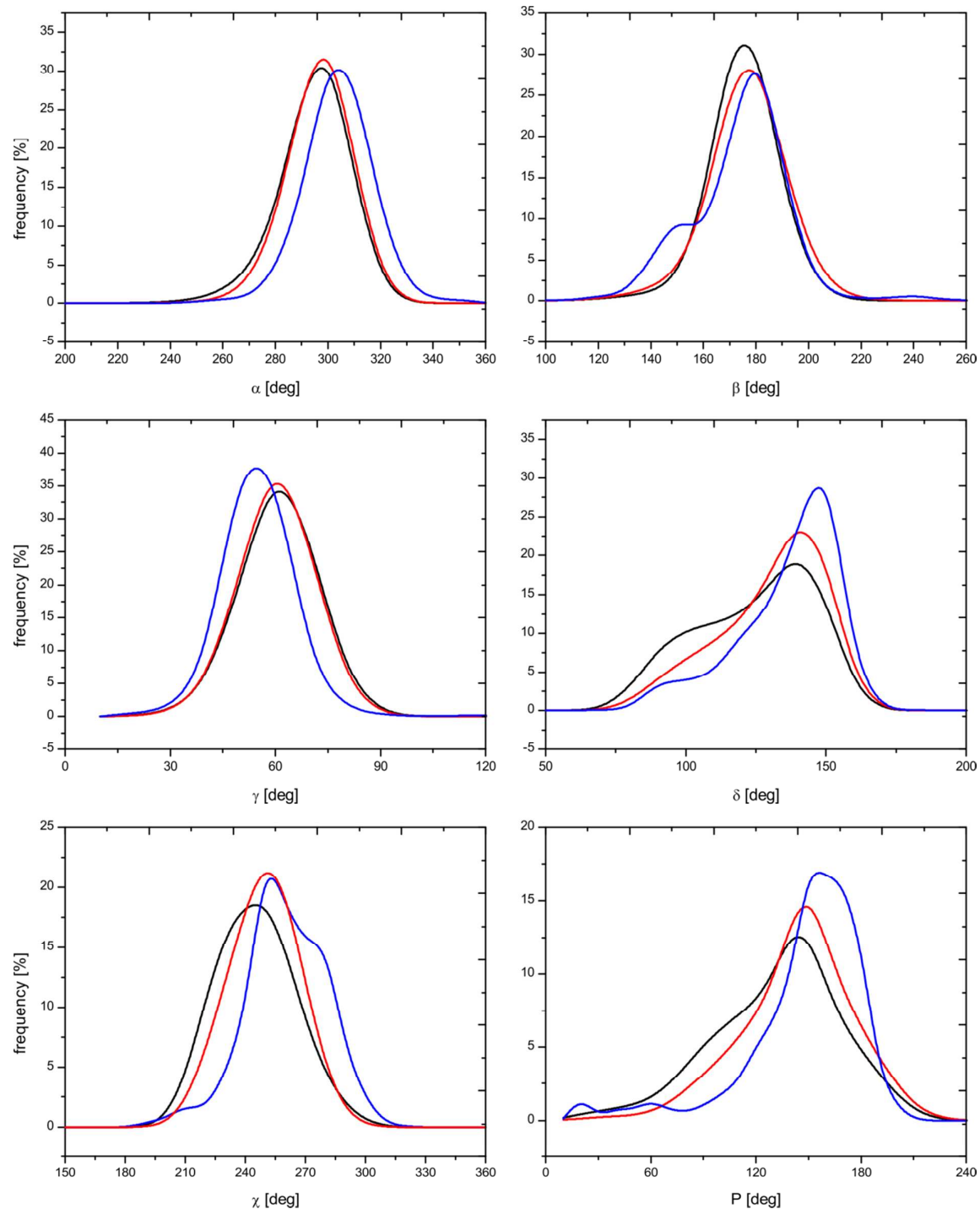
Figure S6. Examples of noncanonical end structure observed in MD simulation of DD with ff99bsc0 force field (trans Watson-Creek/Sugar Edge, cis C-H-Edge/Hoogsteen and stacked structure). See also Drsata et al. *J. Chem. Theory Comput.* **2013,** *9* (1), 707-721.
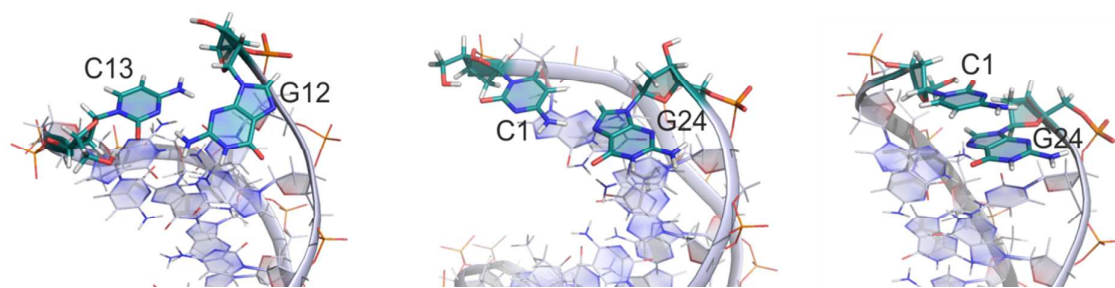
Figure S7. Convergence of ε/ζ flips in the DD dodecamer. BI fraction (cumulative average) as a function of time. Results from 1 μs simulations of DD dodecamer in ff99bsc0 (black) and ff99bsc0εζ$_{OL1}$ (red) force fields.
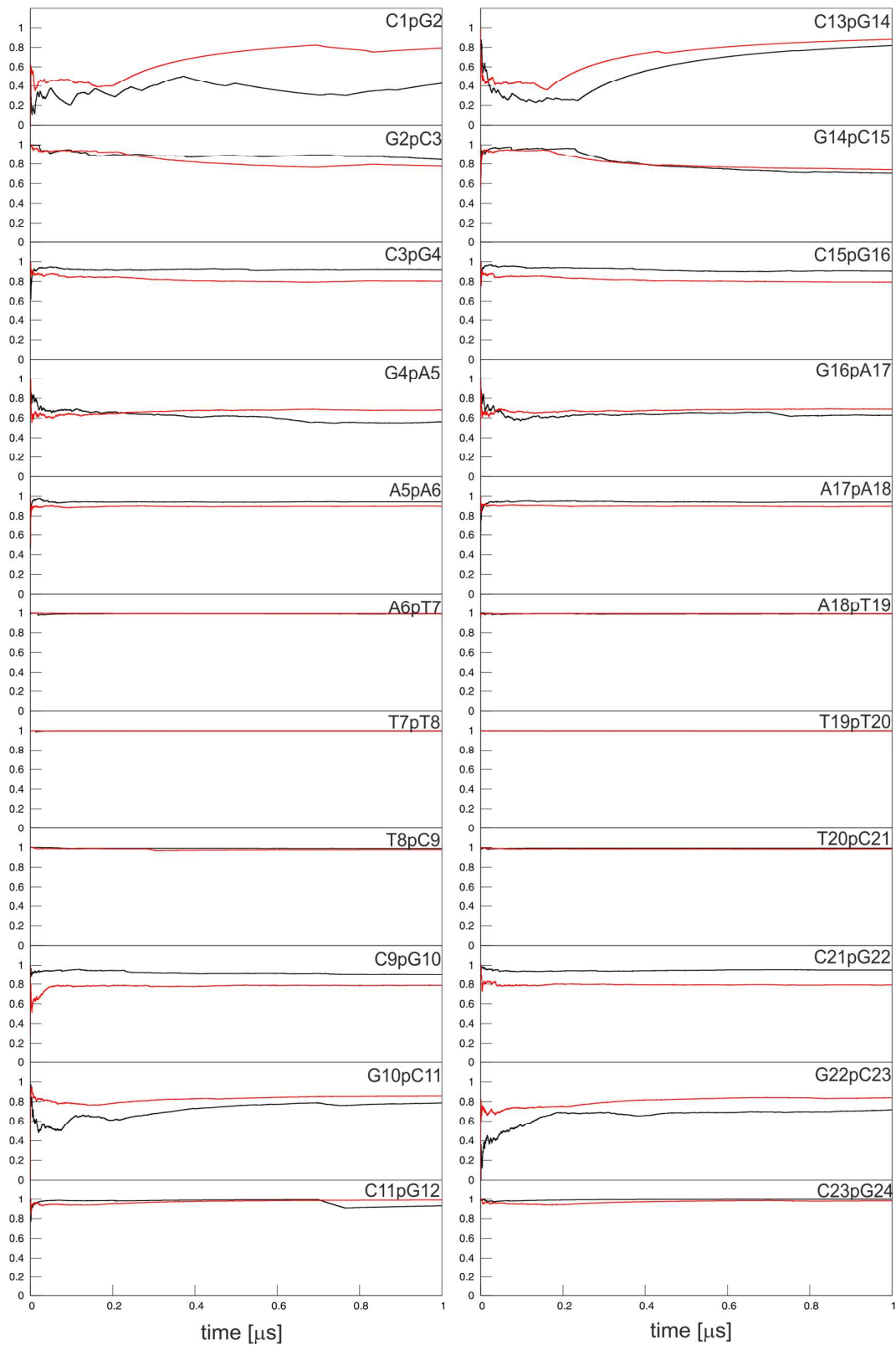
Figure S8. Time evolution of ε–ζ in one strand of the DD dodecamer. Results from 1 μs MD simulation and ff99bsc0 force field. BI is characterized by ε–ζ < 0 and BII by ε–ζ > 0.
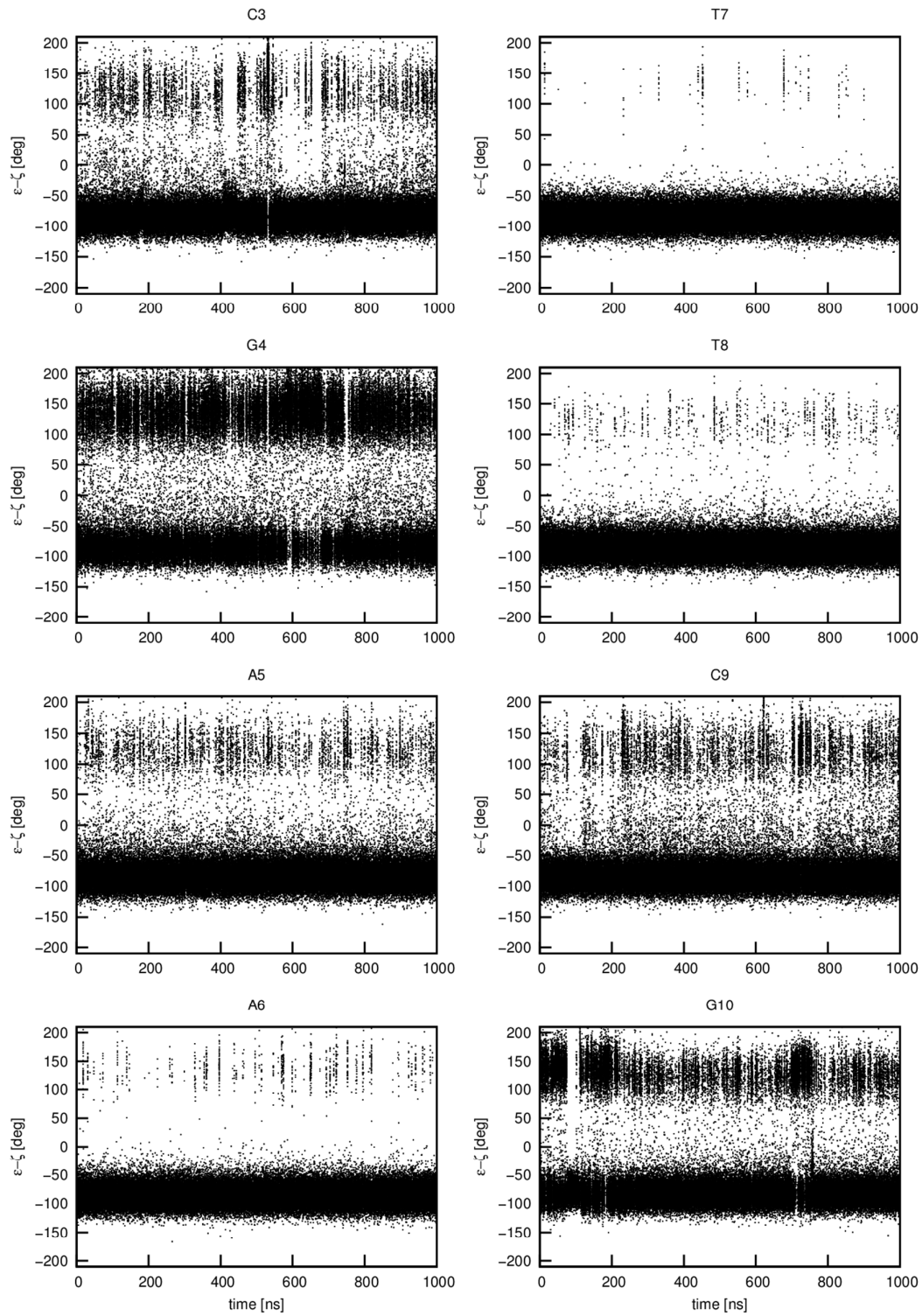
Figure S9. Time evolution of ε–ζ in one strand of the DD dodecamer. Results from 1 μs MD simulation and ff99bsc0εζ$_{OL1}$ force field. BI is characterized by ε–ζ < 0 and BII by ε–ζ > 0.
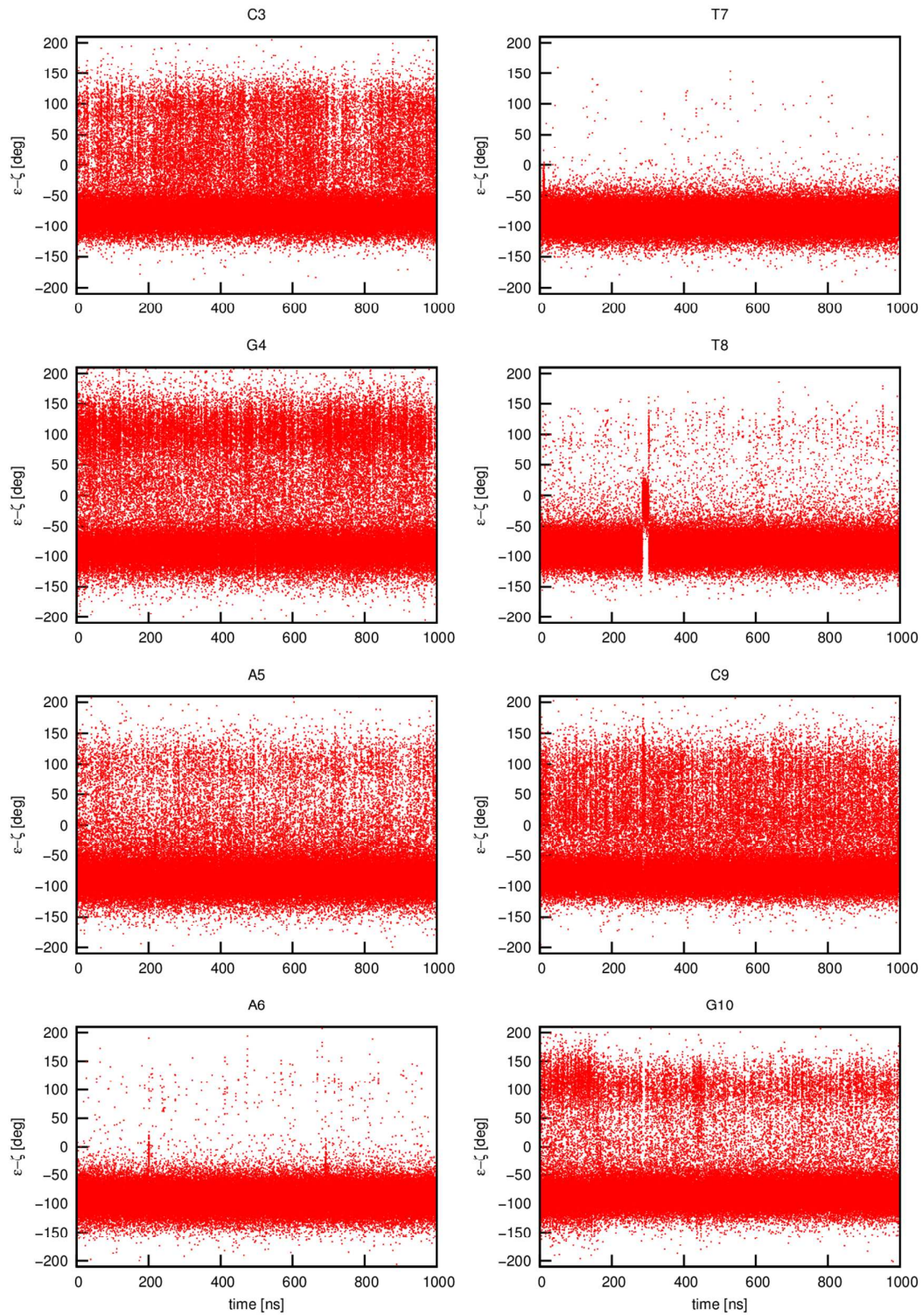
Figure S10. BII fractions for different base steps in the DD dodecamer observed in NMR (green, Schwieters and Clore *Biochemistry* **2007**, *46* (5), 1152-1166) and in ff99bsc0 (black) and ff99bsc0εζ_{OL1} (red) MD simulations compared with CHARMM36 results (gray, taken from Hart et al. *J. Chem. Theory Comput.* **2012,** *8* (1), 348-362)
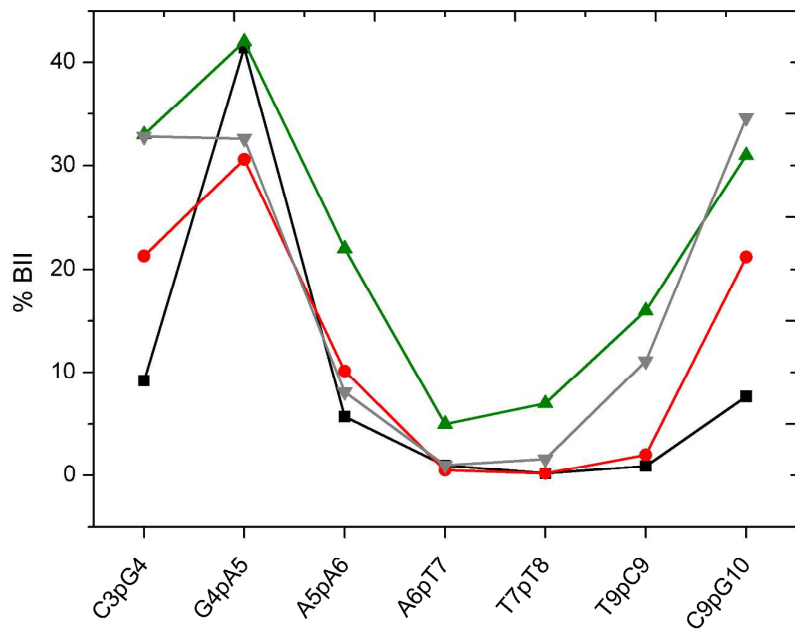
Figure S11. Selected helical parameters for individual base pair steps in the DD dodecamer from MD simulations with ff99bsc0 (black), ff99bsc0εζ$_{OL1}$ (red) and CHARMM36 (gray, taken from Hart et al. *J. Chem. Theory Comput.* **2012,** *8* (1), 348-362) force fields compared with NMR reference (green, 1NAJ structure).
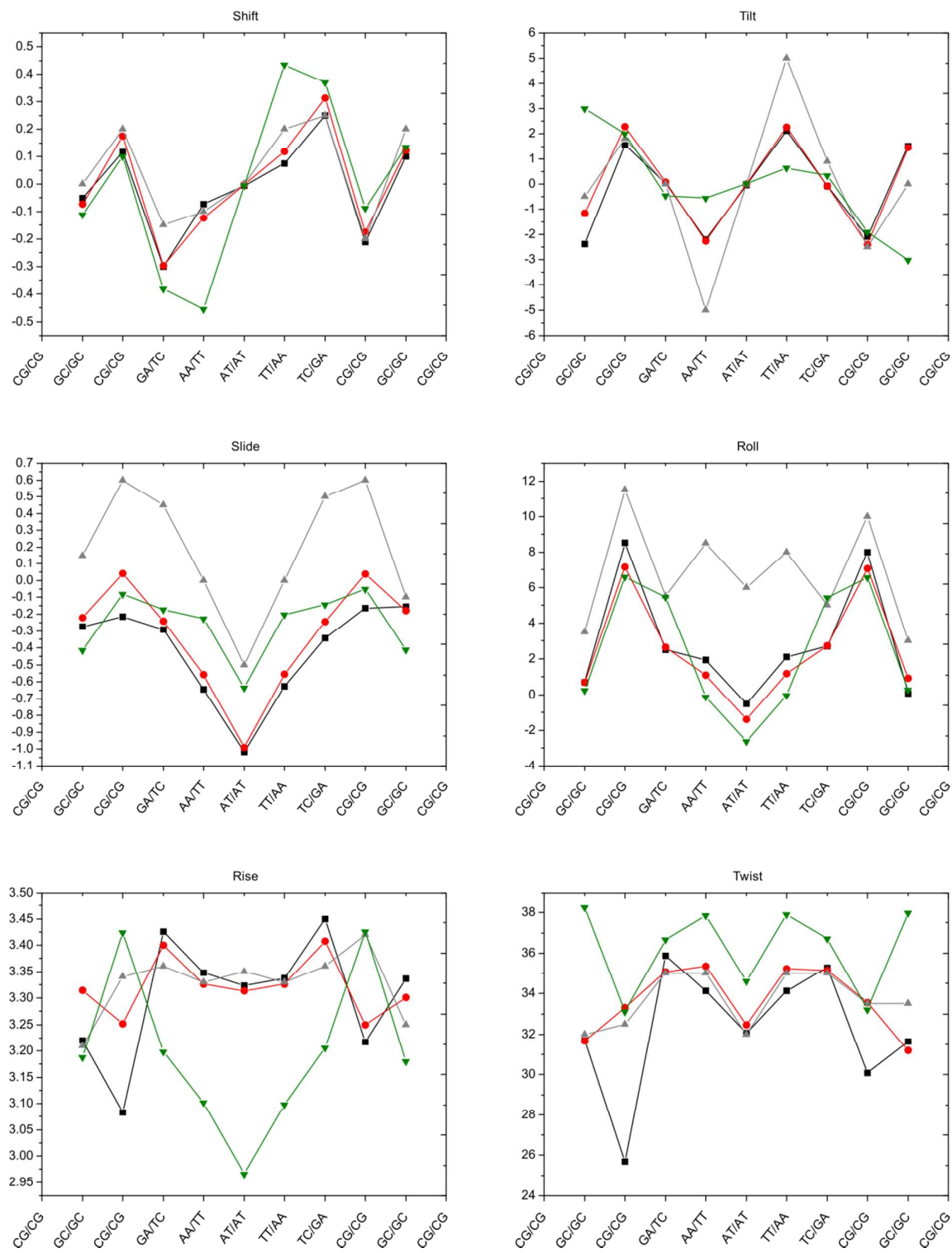
Table S3. Average structural parameters (last 300 ns of 500ns simulations) for the Dickerson-Drew dodecamer. Comparison of ff99bsc0εζ_{OL1} parameters with different water models (TIP3P and SPC/E).

|	X-ray (NMR)	ff99bsc0εζ_{OL1} TIP3P	ff99bsc0εζ_{OL1} SPC/E
minor groove width/ Å	9.9 (10.5)	11.1	10.9
major groove width/ Å	18.0 (17.6)	18.6	18.1
χ/deg	-113.6 (-110.8)	-115.7	-113.6
α/deg	-63.5 (-61.6)	-68.4	-68.9
β/deg	176.1 (173.5)	176.2	176.3
γ/deg	52.9 (50.3)	55.3	55.0
δ/deg	120.4 (126.7)	125.4	127.8
ε/deg	-181.5 (-171.6)	-176.2	-176.3
ζ/deg	-88.7 (-101.3)	-92.8	-93.3
P/deg	130.0 (136.8)	138.0	141.4
tm/deg	37.4 (33.4)	37.4	37.4
shift/ Å	0.0 (0.0)	0.0	0.0
slide/ Å	-0.08 (-0.2)	-0.4	-0.2
rise/ Å	3.3 (3.2)	3.3	3.3
tilt/deg	-0.3 (0.0)	0.0	-0.1
roll/deg	1.9 (3.0)	2.9	2.6
twist/deg	33.6 (35.7)	34.3	34.9
shear/ Å	-0.0 (0.0)	0.0	0.0
buckle/deg	1.2 (0.0)	0.0	-0.2
stretch/ Å	0.0 (-0.3)	0.0	0.0
propeller/deg	-11.4 (-17.5)	-11.8	-11.9
stagger/ Å	0.1 (-0.1)	0.0	0.0
opening/deg	1.8 (-1.1)	0.0	0.0
X-displacement/ Å	-0.5 (-0.8)	-1.2	-0.9
Y-displacement/ Å	-0.1 (0.0)	0.0	0.0
helical rise/ Å	3.3 (3.2)	3.3	3.3
inclination/deg	4.1 (5.0)	5.1	4.6
tip/deg	0.6 (0.0)	0.0	0.2
helical twist/deg	34.0 (36.1)	35.3	35.9
Number of flips/1ns		231	234
%BII		12.0	15.6
RMSD (all)/Å[a]		1.4	1.4
RMSD (backbone)/Å[a]		1.6	1.5

[c]RMSD for all atoms and backbone calculated against 1BNA structure. Two terminal steps are excluded from the calculation of RMSD. RMSD is mass weighted.

Table S4. Average structural parameters (last 800 ns of 1μs simulations) for the Jun-Fos model. Comparison of the ff99bsc0 and ff99bsc0εζ$_{OL1}$ force fields. Two terminal base pairs are excluded from the analysis.

	ff99bsc0	ff99bsc0εζ$_{OL1}$
minor groove width/ Å	11.9	11.7
major groove width/ Å	20.6	20.9
χ/deg	-125.0	-123.0
α/deg	-69.4	-67.6
β/deg	174.6	177.1
γ/deg	56.7	55.9
δ/deg	119.2	121.0
ε/deg	-173.9	-177.2
ζ/deg	-89.5	-91.4
P/deg	126.7	131.1
tm/deg	37.5	37.7
shift/ Å	0.0	0.0
slide/ Å	-0.7	-0.8
rise/ Å	3.4	3.5
tilt/deg	0.1	0.1
roll/deg	-0.5	-0.5
twist/deg	32.7	32.5
shear/ Å	0.0	0.0
buckle/deg	-2.1	-1.3
stretch/ Å	0.0	0.0
propeller/deg	-9.5	-7.9
stagger/ Å	0.0	0.0
opening/deg	0.3	0.3
X-displacement/ Å	-1.3	-1.6
Y-displacement/ Å	0.0	0.0
helical rise/ Å	3.4	3.4
inclination/deg	-0.2	-0.5
tip/deg	-0.2	-0.1
helical twist/deg	33.6	33.4
%BII	11.0	10.0

Table S5. Average structural parameters (last 800 ns of 1 μs simulations) for the d(CCCCCGGGGG)$_2$ (C$_5$G$_5$) structure. Comparison of the ff99bsc0 and ff99bsc0εζ_{OL1} force fields.

	ff99bsc0	ff99bsc0εζ_{OL1}
minor groove width/ Å	13.7	13.4
major groove width/ Å	20.5	19.5
χ/deg	-130.2	-121.4
α/deg	-71.0	-70.7
β/deg	174.6	176.0
γ/deg	56.6	55.2
δ/deg	112.9	122.4
ε/deg	-172.4	-173.7
ζ/deg	-88.3	-91.9
P/deg	117.8	132.7
tm/deg	38.4	38.1
shift/ Å	0.0	0.0
slide/ Å	-1.1	-0.7
rise/ Å	3.4	3.4
tilt/deg	-0.1	0.1
roll/deg	5.3	4.2
twist/deg	30.1	31.6
shear/ Å	0.0	0.0
buckle/deg	0.8	-1.2
stretch/ Å	-0.1	-0.1
propeller/deg	-5.4	-5.3
stagger/ Å	-0.1	-0.1
opening/deg	-0.3	-0.3
X-displacement/ Å	-3.2	-2.2
Y-displacement/ Å	0.0	0.0
helical rise/ Å	3.1	3.2
inclination/deg	10.3	8.0
tip/deg	0.2	-0.3
helical twist/deg	31.4	32.7
% BII	4.0	11.5

Table S6. Average structural parameters (last 800 ns of 1μs simulations) for the short A-tract (A_3T_3) structure (PDB ID 1S2R). Comparison of the ff99bsc0 and ff99bsc0εζ_{OL1} force fields. Two terminal base pairs are excluded from the analysis.

	X-ray	ff99bsc0	ff99bsc0εζ_{OL1}
minor groove width/ Å	9.7	11.4	11.0
major groove width/ Å	18.3	19.9	18.9
χ/deg	-112.7	-119.5	-117.0
α/deg	-58.1	-70.2	-68.1
β/deg	172.9	174.3	176.3
γ/deg	54.9	55.8	55.5
δ/deg	121.6	118.3	122.9
ε/deg	-179.2	-173.1	-176.8
ζ/deg	-94.4	-88.6	-91.8
P/deg	132.5	124.8	133.4
tm/deg	35.7	38.1	37.7
shift/ Å	0.0	0.0	0.0
slide/ Å	0.1	-0.5	-0.5
rise/ Å	3.3	3.4	3.3
tilt/deg	0.4	0.0	0.0
roll/deg	0.7	4.0	3.0
twist/deg	34.4	31.5	33.3
shear/ Å	0.0	0.0	0.0
buckle/deg	2.2	-0.2	-0.1
stretch/ Å	0.0	0.0	0.0
propeller/deg	-13.2	-11.8	-12.1
stagger/ Å	0.2	0.0	0.0
opening/deg	2.8	0.9	0.6
X-displacement/ Å	0.0	-1.9	-1.5
Y-displacement/ Å	0.0	0.0	0.0
helical rise/ Å	3.3	3.2	3.2
inclination/deg	1.9	8.5	5.6
tip/deg	-0.6	-0.1	0.0
helical twist/deg	34.7	32.9	34.4
%BII		7.7	8.5
rmsd (all)/Å		2.0	1.7
rmsd(backbone)/Å		2.2	1.8

Table S7. Average structural parameters (last 800 ns of 1μs simulations) for A-tract (A_6) structure (PDB ID 1D89). Comparison of the ff99bsc0 and ff99bsc0$\varepsilon\zeta_{OL1}$ force fields. Two terminal base pairs are excluded from the analysis.

	X-ray	ff99bsc0	ff99bsc0$\varepsilon\zeta_{OL1}$
minor groove width/ Å	9.6	11.5	11.1
major groove width/ Å	17.8	19.6	19.1
χ/deg	-113.1	-121.6	-117.3
α/deg	-68.4	-69.0	-67.5
β/deg	175.9	174.1	176.2
γ/deg	60.0	56.4	55.8
δ/deg	128.9	118.6	123.6
ε/deg	-179.1	-174.1	-177.2
ζ/deg	-101.3	-89.9	-92.5
P/deg	139.5	126.6	135.3
tm/deg	40.6	37.5	37.3
shift/ Å	0.0	-0.1	-0.1
slide/ Å	-0.1	-0.5	-0.4
rise/ Å	3.2	3.3	3.3
tilt/deg	-0.6	-0.5	-0.5
roll/deg	0.4	3.0	2.1
twist/deg	34.9	33.1	34.2
shear/ Å	0.0	0.1	0.1
buckle/deg	1.8	2.6	3.1
stretch/ Å	-0.3	0.0	0.0
propeller/deg	-16.2	-13.2	-12.8
stagger/ Å	0.1	0.0	0.0
opening/deg	1.6	0.5	0.5
X-displacement/ Å	-0.2	-1.6	-1.2
Y-displacement/ Å	0.1	0.0	0.1
helical rise/ Å	3.2	3.2	3.3
inclination/deg	0.9	5.7	3.8
tip/deg	1.1	0.8	0.7
helical twist/deg	35.4	34.1	35.1
%BII		7.4	9.5
rmsd (all)/Å		1.8	1.5
rmsd (backbone)/Å		2.0	1.6

Table S8. Average structural parameters (last 800 ns of 1μs simulations) for AT rich (3AT) structure. Comparison of the ff99bsc0 and ff99bsc0εζ_{OL1} force fields. Two terminal base pairs are excluded from the analysis.

	ff99bsc0	ff99bsc0εζ_{OL1}
minor groove width/ Å	12.7	11.9
major groove width/ Å	19.4	19.1
χ/deg	-123.9	-118.1
α/deg	-69.7	-68.9
β/deg	174.2	176.5
γ/deg	56.6	55.6
δ/deg	115.1	122.8
ε/deg	-173.1	-175.9
ζ/deg	-88.7	-92.5
P/deg	120.7	133.9
tm/deg	37.8	37.7
shift/ Å	0.0	0.0
slide/ Å	-0.8	-0.6
rise/ Å	3.3	3.3
tilt/deg	0.0	0.0
roll/deg	6.4	4.4
twist/deg	31.2	33.0
shear/ Å	0.0	0.0
buckle/deg	0.4	-0.1
stretch/ Å	0.0	0.0
propeller/deg	-12.0	-10.9
stagger/ Å	0.0	0.0
opening/deg	1.2	1.0
X-displacement/ Å	-2.5	-1.8
Y-displacement/ Å	0.0	0.0
helical rise/ Å	3.0	3.1
inclination/deg	11.6	7.6
tip/deg	-0.1	0.0
helical twist/deg	33.1	34.3
%BII	3.1	7.7

Table S9. Average structural parameters (last 300 ns of 500ns simulations) for the A-RNA duplex 1QC0' (r(GCACCGUUGG)) obtained using ff99bsc0χ_{OL3} and ff99bsc0$\chi_{OL3}\epsilon\zeta_{OL1}$ force fields.

	X-ray	99bsc0χ_{OL3}	99bsc0$\chi_{OL3}\epsilon\zeta_{OL1}$
minor groove width/Å	15.4	15.3	15.3
major groove with/Å	14.7	17.8	17.7
χ/deg	-163.0	-160.7	-160.3
α/deg	-65.7	-75.5	-74.8
β/deg	170.6	174.0	173.1
γ/deg	56.7	63.9	63.7
δ/deg	79.4	77.9	78.7
ϵ/deg	-152.4	-158.5	-156.4
ζ/deg	-71.6	-68.2	-70.3
P/deg	17.7	16.5	17.9
tm/deg	44.9	40.1	39.9
shift/ Å	-0.1	0.0	0.0
slide/ Å	-1.7	-1.9	-1.9
rise/ Å	3.2	3.4	3.4
tilt/deg	-1.2	0.2	0.2
roll/deg	8.1	6.7	7.5
twist/deg	30.8	28.8	28.8
shear/ Å	0.1	0.0	0.0
buckle/deg	1.2	0.9	1.9
stretch/ Å	-0.3	0.0	0.0
propeller/deg	-12.5	-9.9	-9.9
stagger/ Å	0.1	-0.2	-0.2
opening/deg	1.4	0.8	1.3
X-displacement/ Å	-4.5	-4.9	-5.0
Y-displacement/ Å	-0.1	0.0	0.0
helical rise/ Å	2.6	2.8	2.8
inclination/deg	15.2	12.7	14.2
tip/deg	2.1	-0.5	-0.3
helical twist/deg	32.3	30.4	30.7
rmsd(all)/Å		1.1	1.2
rmsd(backbone)/Å		1.1	1.2